JOURNAL OF SOLID STATE CHEMISTRY 113, 54–61 (1994)

Solid State Chemistry of New Perovskite and Ruddlesden–Popper Phases in the La_2O_3–CaO–CuO System at High Pressures

Arnold M. Guloy,[1] Bruce A. Scott, and Richard A. Figat

IBM Research Division, Thomas J. Watson Research Center, P.O. Box 218, Yorktown Heights, New York 10598

Received November 19, 1993; in revised form January 24, 1994; accepted January 26, 1994

The crystal chemistry of the system $LaO_{1.5}$–CaO–CuO at the 1:1:2 composition was studied at high pressures with the goal of stabilizing new perovskite cuprates with two-dimensional ordering of La, Ca cations and oxygen vacancies. Several phases, including the perovskites $La_4Ca_4Cu_8O_{20}$, $La_4Ca_4Cu_{88}O_{18}$ and the Ruddlesden–Popper (RP) phase $La_2Ca_2Cu_3O_8$, containing three copper oxide layers ($n = 3$), were revealed for the first time. The results are very sensitive to experimental conditions, and a variety of reaction channels are observed at the 1:1:2 composition depending on the choice of total pressure, p_{O_2}, temperature, and annealing conditions. The perovskite-related phases at this composition exhibited *A*-site cation disorder and three-dimensional ordering of oxygen vacancies. The Ruddlesden–Popper phase required the substitution of Sr on the *A*-sites to be metastably retained at room temperature. Due to its thermal instability, the RP phase could not be doped to a carrier concentration at which superconductivity might be observed.

INTRODUCTION

High pressure methods are promising for the possible preparation of new high temperature cuprate superconductors (1, 2). High T_c materials exhibit structures derived in some way from ABO_3 perovskite, a high density structure stabilized by the large increase in electrostatic Madelung energy occurring with decreasing unit cell volume, provided, of course, that repulsive interactions do not begin to dominate (2, 3). As a result, it becomes possible to place cations in higher coordination geometries than those found in lower pressure phases. For example, silicon coordination changes from tetrahedral to octahedral in pyroxene minerals as they transform to perovskites at the higher pressures and temperatures of the earth's mantle (4). Many of these transformations, as well as new synthetic materials, can be quenched from these extreme conditions and kinetically retained at ambient pressure. We have found that cuprate perovskites so prepared can often be heated to temperatures above 800°C at atmospheric pressure before complete decomposition occurs. In principle, such metastable "precursors" can be processed further under milder P–T–p_{O_2} conditions to obtain phases with specific cation and oxygen vacancy orderings. This is a strategy we have adopted in attempting to synthesize certain ordered perovskite-like phases in the present study.

Much recent high pressure synthesis work has focussed on the perovskite-derived $ACuO_2$ infinite-layer structure (5–10). $SrCuO_2$ and a wide range of solid solutions with A = (Sr, Ca) and (Ba, Sr) were synthesized at 1000°C and pressures above 50 kbar using an oxygen buffer. The insulator $Ca_{1-x}Sr_xCuO_2$, with $x = 0.85$–0.9, is the only known cuprate with this lattice type that can be prepared at $P = 1$ bar (11). Superconductivity was observed in several of the high pressure infinite-layer samples (6, 7). Azuma *et al.* (7) measured a T_c onset of 110 K in the *A*-cation deficient composition $(Sr_{0.7}Ca_{0.3})_{0.9}CuO_2$. Confirmation of the structural results and the *p*-type conductivity has been recently presented (12). On the other hand, *n*-type superconductivity with $T_c \approx 40$ K has been found in the infinite-layer $Ln_xSr_{1-x}CuO_2$ systems for Ln = La, Pr, Nd and Sm ($\delta \leq 0.15$). These were synthesized at $T \gtrsim 1000$°C and $P \gtrsim 25$ kbar in the absence of an oxygen buffer (13–15).

A few other high T_c cuprates have also been prepared at these extreme pressures. A Ruddlesden–Popper (RP) phase, $La_{1.7}Ca_{1.3}Cu_2O_6$, analogous to $Sr_3Ti_2O_7$, was synthesized at 60 kbar and 1050°C (16). It exhibited a T_c onset of 70 K. This two-layer RP phase can also be made under much milder conditions (17). Synthesis of the T' structure of Ln_2CuO_4 is limited to Ln = Nd–Gd at ambient pressure (18, 19), but this lattice-type can be stabilized for the smaller Ln = Y, Tb, Dy, Ho, Er, and Tm at $P \gtrsim 60$ kbar (20, 21).

Previous work from this laboratory at $p_{O_2} = 1$ kbar has revealed a rich structural chemistry of ordered oxygen vacancy phases in the $LaCuO_{3-\delta}$ perovskite system (22, 23). In tbe present investigation, these studies have been extended to much higher pressures with the intention of

[1] Present address: Department of Chemistry, University of Houston, Houston, TX 77204-5641.

0022-4596/94 $6.00

creating a well-defined homologous series between the perovskite and infinite-layer structures. In our initial work we have attempted to prepare the simplest example of such a material: cation- and oxygen-vacancy-ordered phases of the $YBaFeCuO_5$ structure type (24–26). The results of these investigations, focusing on coupled La and Ca chemistry at high pressures, are presented herein.

EXPERIMENTAL

Reaction mixtures for the high P, T synthesis were prepared from nitrate precursors. The rare-earth oxides (99.99%, prefired at 950°C for 12 hr), an alkaline-earth carbonate ($CaCO_3$, $SrCO_3$) and CuO in the desired stoichiometry were dissolved in 0.5 M HNO_3. The resulting blue solution was slowly evaporated to dryness in teflon boats with intermittent stirring to maximize the homogeneity of the nitrate mixture, which was then dried overnight at 120°C. The dried cake was then ground, placed in Pt containers and decomposed under flowing oxygen by slow heating from 200 to 750°C. Mixtures were held at that temperature for 6 hr before cooling to room temperature, and the resulting black precursors were stored in a desiccator before use.

The high P, T reactions were performed in a girdle-type system using a 300-ton automated press (Pressure Systems Research Inc.). The girdle consists of a cylindrical arrangement of hardened steel rings confining a central 11/16"-i.d. tungsten carbide core which holds the sample assembly. Pressurization is achieved by forcing a pair of tungsten carbide anvils against the assembly, which is fabricated from a pyrophyllite cylinder 17 mm in diameter and 12 mm long. A 9-mm-diameter hole through the length of the pyrophyllite is fitted with a hollow graphite heating element surrounded by alumina sleeves. The reaction mixture (50–100 mg), packed into a 4-mm-long cold-sealed Pt tube, is centered within the assembly using alumina rods. The graphite tube is heated by an electric current through contact with the WC pistons. Temperatures from 550 to 1100°C were maintained ±5°C for the desired period using a Eurotherm power controller and Pt/Pt–10Rh thermocouple. A source of oxygen was provided by mixing $KClO_3$ directly with the sample. Although this approach leads to the contamination of the product by KCl, it was found to be the most effective means of producing homogeneous phases. Various schemes for separating the $KClO_3$ from the reaction mixture, including the use of thin platinum or zirconia discs, invariably led to incompletely reacted materials, or to composition gradients within the reaction products. No evidence was found for the reaction of KCl in the phase assemblage.

The products were characterized with a Siemens D-500 X-ray powder diffractometer. In most cases there was too little sample to perform a complete Rietveld analysis, and the following approach was too little sample to perform a complete Rietveld analysis, and the following approach was therefore used. Lattice parameters were derived by trial and error refinement using the program TREOR (27) and calculating a model powder pattern using the POWD (28) and LAZY PULVERIX (29) programs. Least-squares refinement of the indexed powder data was performed using LATT (30). Theoretical and experimental X-ray powder patterns were carefully compared to test the viability of the structural models. Confirmation of the lattice symmetry and unit cell parameters was based on electron diffraction on selected samples, using a Phillips EM230, to ensure that the most complete structural model had been obtained. The oxygen content was determined by thermogravimetric analysis (TGA) by heating the samples to decomposition in argon.

RESULTS AND DISCUSSION

Exploratory high pressure studies were conducted with the goal of synthesizing certain 2D-like ordered phases; for example, a cuprate with the $YBaCuFeO_5$ structure (24–26). This structure is a defect perovskite with an alternating arrangement of Y and Ba cations along ⟨001⟩ and ordering of oxygen vacancies into the Y-planes. Oxygens alone separate the double sheets of (Cu, Re)O_2, so that if this phase could be synthesized with only copper in the B-sites, and doped, it would be interesting to contrast its properties to the infinite-layer phases and $YBa_2Cu_3O_7$.

Our initial work concentrated on attempting to prepare the desired structure-type in the systems Y–Ba–Cu–O and Y–Sr–Cu–O. Experiments were conducted at pressures up to 60 kbar and temperatures to 1100°C with the $KClO_3$ content adjusted to obtain the correct stoichiometry. Experiments at the compositions $YBaCu_2O_5$ and $YSrCu_2O_5$ yielded products containing several unknown phases. Analysis of the mixtures by X-ray powder diffractometry showed that none of the phases had perovskite-related structures. Ono found several perovskite-like materials for (Y + Sr)/Cu > 1 at pressures below 20 kbar in the Y–Sr–Cu–O system (9). This result and the fact that we have observed substantial changes in the X-ray powder patterns with changes in p_{O_2} and total pressure, indicate that many new and unknown phases occur in both the Y–Sr–Cu–O and Y–Ba–Cu–O systems at high pressure.

The $YBaCuFeO_5$ structure type can be considered an ordered intercalation of the $A'BO_2$ infinite-layer structure into an ABO_3 perovskite. Given the complexity of these multicomponent systems in phase space, it was decided to examine the high pressure reactions of $Ca_{0.85}Sr_{0.15}CuO_2$ with $LaCuO_3$, i.e., a pseudo-system comprised of end members with these respective structures. A series of reactions was carried out at the composition La

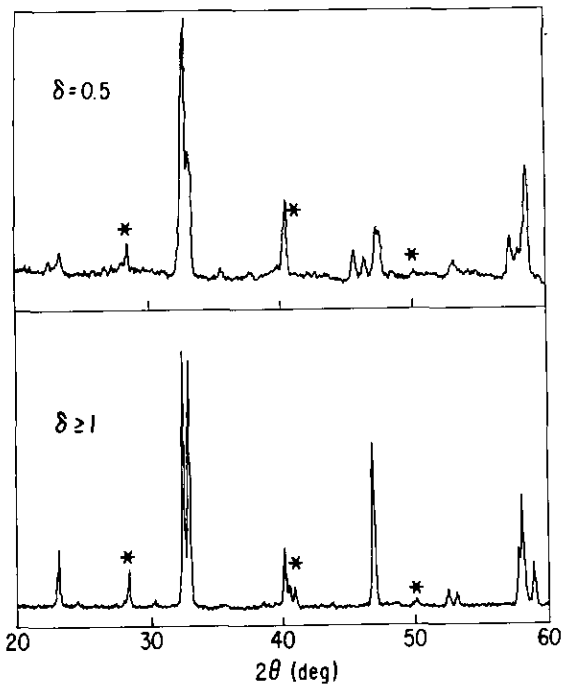

FIG. 1. X-ray powder patterns of $LaSr_{0.15}Ca_{0.85}Cu_2O_{4.5+\delta}$ for $\delta = 0.5$ and 1.0 (nominal). Asterisks denote KCl reflections.

$Ca_{0.85}Sr_{0.15}Cu_2O_{4.5+\delta}$, where nominally, $\delta = 0$ for p_{O_2} = 1 bar. For $KClO_3$ contents corresponding to $\delta = 0.5$, quenching the reaction mixture after 2 hr at 1025°C and 60 kbar pressure gave a single phase material with the tetragonal $LaCuO_3$ structure (22). On the other hand, under the same reaction and quenching conditions, the rhombohedral $LaCuO_3$ structure (31) occurred when the buffer content was increased to make the nominal $\delta \geq 1$. The X-ray diffraction patterns of the two product phases are shown in Fig. 1. Annealing experiments carried out at 100 kbar and 650°C did not yield the desired *A*-site-ordered phase. On heating to 1000°C at p_{O_2} = 1 bar, both the tetragonal and rhombohedral phases transformed to the orthorhombic $La_2Cu_2O_5$ structure (22), the latter with the loss of oxygen, prior to complete decomposition. Studies are underway using a wider range of annealing conditions to determine whether *A*-site cation ordering into a $YBaFeCuO_5$-type or related structure can be induced. It is interesting to note that the +2.5 average oxidation state of copper in tetragonal $LaCa_{.85}Sr_{.15}Cu_2O_5$ is very close to that in $LaCuO_{2.8}$, the composition defining the lower limit of tetragonal phase stability in the $LaCuO_{3-\delta}$ system (22, 23).

Simplification by removing strontium from the reaction mixture led to completely different results. X-ray powder diffraction of the product of composition $LaCaCu_2O_{5+\delta}$ ($KClO_3$ corresponding to nominal $\delta = 0.5$ or 1.0), quenched from 60 kbar and 1025°C, revealed a tetragonal cell, related to a simple perovskite cell by $a = 2\sqrt{2}\, a_p$ and $c = a_p$. All the observed X-ray powder diffraction lines were indexed to a cell with dimensions $a = 10.727(1)$ and $c = 3.797(2)$ Å, isotypic with $La_{8-x}Sr_xCu_8O_{20}$ ($1.28 < x < 1.92$) (32). The actual stoichiometry is $La_4Ca_4Cu_8O_{20+\delta}$, with $\delta = 0.3$. This is based on TGA experiments corrected for the amount of KCl present, which is known from the $KClO_3$ concentration in the original charge. TGA showed that the oxygen content is always close to 20 provided that enough buffer is added to the reaction mixture to insure that the nominal $\delta \geq 0.5$.

Electron diffraction studies on $La_4Ca_4Cu_8O_{20+\delta}$ confirmed the tetragonal symmetry and cell dimensions derived from X-ray powder diffraction, as well as the reflection condition $0kl$ with $k = 2n$, which is consistent with space group $P4/mbm$. Contrary to the results reported by Er-Rakho *et al.* (32) on $La_{8-\delta}Sr_\delta Cu_8O_{20}$, our electron diffraction experiments on many sample crystallites showed no evidence of a superstructure along ⟨001⟩. In addition, EDAX measurements on representative crystallites proved them to be free of K or Cl impurities.

The X-ray powder pattern of $La_4Ca_4Cu_8O_{20+\delta}$ is given in Table 1, and a full view of the structure, at an 8° tilt

TABLE 1
Powder X-Ray Diffraction Pattern of $La_4Ca_4Cu_8O_{20+\delta}$
($a = 10.727(1)$; $c = 3.797(2)$ Å)

d_{obs}	d_{calc}	I_o	I_c	h	k	l
3.7968	3.797	10	8	0	0	1
	3.7936	10	10	2	2	0
	3.3931	—	1	1	1	1
2.9779	2.9776	10	8	2	1	1
2.6822	2.6837	100	100	2	2	1
	2.6825	50	48	4	0	0
2.6033	2.6024	30	17	4	1	0
	2.5301	—	1	3	1	1
2.5265	2.5291	5	2	3	3	0
2.4004	2.3993	5	2	4	2	0
2.3408	2.3423	10	12	3	2	1
2.1927	2.1909	20	15	4	0	1
2.1465	2.1466	30	12	4	1	1
	2.1460	—	15	4	3	0
	2.1049	—	1	3	3	1
	2.1043	—	1	5	1	0
1.8970	1.8985	30	17	0	0	2
	1.8968	—	17	4	4	0
1.8410	1.8406	5	3	5	1	1
	1.8402	2	2	5	3	0
	1.6978	—	1	2	2	2
	1.6969	—	1	4	4	1
1.6753	1.6757	5	5	5	4	0
1.5997	1.5998	10	9	6	1	1
	1.5995	—	2	6	3	0
1.5492	1.5497	20	15	4	0	2
	1.5490	15	16	6	2	1

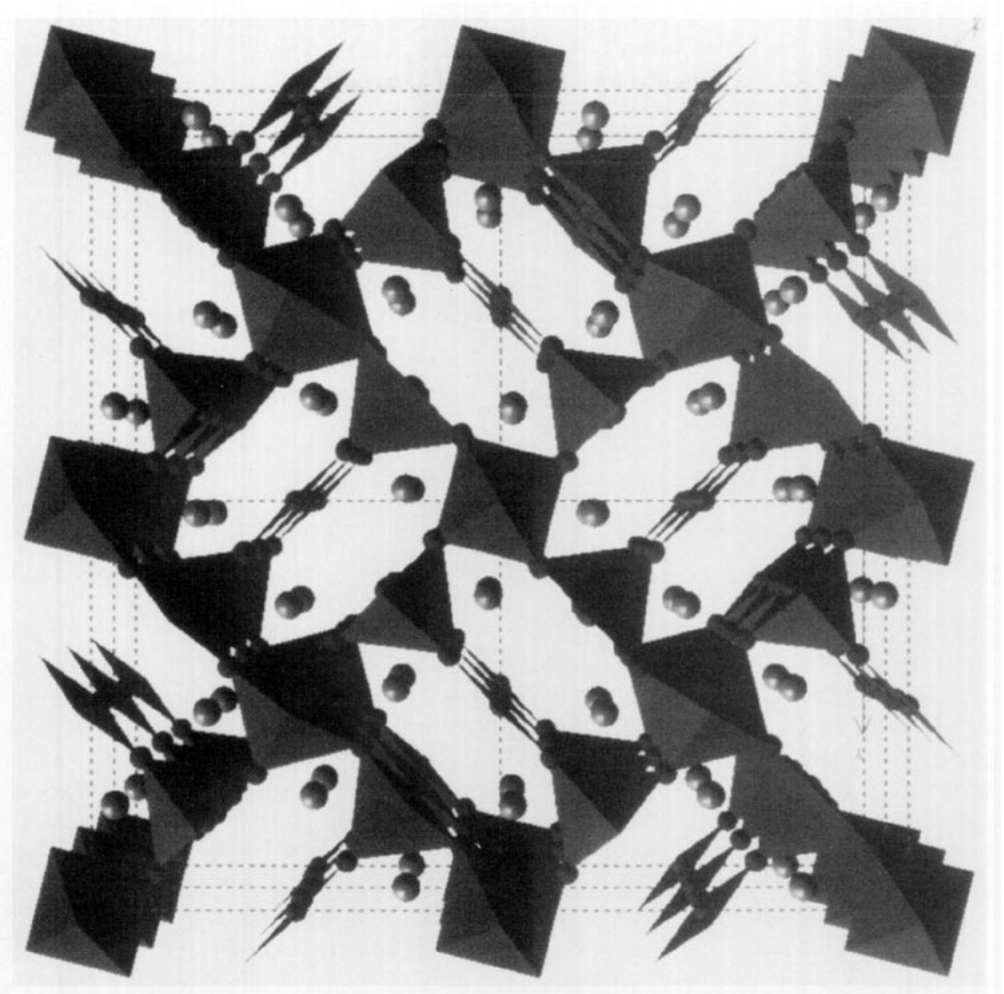

FIG. 2. Three dimensional representation of the $La_4Ca_4Cu_4O_{20}$ structure, tilted 8° off ⟨001⟩, showing disordered La/Ca cations in the hexagonal channels and 4-, 5-, and 6-fold Cu–O coordination polyhedra.

off ⟨001⟩, is presented in Fig. 2. The structure can be described as an oxygen-deficient perovskite whose superlattice arises from oxygen vacancy ordering, with La, Ca cations randomly distributed in the *A*-type sites. This lattice shows similarities to the structure of $La_4BaCu_5O_{13+\delta}$ (33), and $LaCuO_{2.6}$ (22). In both structures, groups of four square pyramidal CuO_5 units share corners with one octahedral CuO_6 unit to create a framework of hexagonal tunnels in three dimensions. However, the (Cu_5O_{22}) groups are arranged in a different way, resulting in double hexagonal channels in $La_4Ca_4Cu_8O_{20+\delta}$ and single channels in $La_4BaCu_5O_{13+\delta}$ and $LaCuO_{2.6}$. Hexagonal channels are also observed in the perovskite-derived, orthorhombic $La_2Cu_2O_5$, but here the octahedral CuO_6 fragment is missing, and the absence of the square unit leads to lower symmetry.

As in the previous case, annealing experiments carried out under different atmospheres (Ar and O_2) did not lead to ordering of the La and Ca cations in $La_4Ca_4Cu_8O_{20.3}$, but an interesting transformation was observed. The TGA profile under flowing oxygen from room temperature to 850°C showed two constant weight plateaus at 300 and 650°C, the net change corresponding to the formation of a new reduced phase:

$$La_4Ca_4Cu_8O_{20+\delta} \rightarrow La_4Ca_4Cu_8O_{18} + (2 + \delta)/2O_2. \quad [1]$$

Based on careful indexing of its X-ray powder pattern, which is shown in Table 2, $La_4Ca_4Cu_8O_{18}$ was found to be tetragonal with $a = 10.738(2)$ and $c = 3.726(1)$ Å, and isostructural with $La_2Sr_6Cu_8O_{18-\delta}$ (34). The reduced phase is also an ordered defect perovskite, easily derived from $La_4Ca_4Cu_8O_{20+\delta}$. In both structures, oxygen vacancies in the basal plane are ordered in the same way along (001), forming identical hexagonal tunnels running along the *c*-axis. However, the differences between them arises from the extra oxygen vacancies in $La_4Ca_4Cu_8O_{18}$, which are also ordered in the $x = 1/2$ plane along (110). The

TABLE 2
Powder X-Ray Diffraction Pattern of $La_4Ca_4Cu_8O_{18}$
(a = 10.738(2); c = 3.726(1) Å)

d_{obs}	d_{calc}	I_o	I_c	h	k	l
4.803	4.8022	2	2	2	1	0
3.800	3.7965	1	1	2	2	0
	3.3957	—	1	1	1	2
	2.9438	—	3	2	1	1
2.685	2.6845	50	46	1	1	3
2.660	2.6592	100	100	2	2	1
2.601	2.6043	10	10	4	1	0
2.323	2.3264	5	7	3	2	1
2.180	2.1781	5	7	4	0	1
1.863	1.8630	15	15	0	0	2
1.670	1.6670	2	3	5	4	0
1.595	1.5953	5	6	6	6	1
1.545	1.5450	20	23	6	2	1

oxygen vacancies created in $La_4Ca_4Cu_8O_{18}$ are associated with the CuO_6 octahedral units in $La_4Ca_4Cu_8O_{20+\delta}$, consistent with the more oxidized nature of Cu in octahedral vs square pyramidal and square planar coordination. Hence, upon reduction, oxygen is eliminated from this site. In Fig. 2, the (Cu_8O_{18}) framework in $La_4Ca_4Cu_8O_{18}$ is built of corner-sharing CuO_4 square planes and CuO_5 square pyramids, whereas in $La_4Ca_4Cu_8O_{20}$, the (Cu_8O_{20}) framework consists of these features plus CuO_6 octahedra. Furthermore, there are two different CuO_4 square planes, one is linked to 4 CuO_5 pyramids, the other is connected to two CuO_5 pyramids, where the CuO_4 planes are perpendicular and parallel to the c-axis, respectively.

The average copper valence is +2.5 in $La_4Ca_4Cu_8O_{20}$, resulting in a mixed valence metallic phase. Superconductivity was not observed, however, in ac susceptibility measurements down to 4 K. Lack of high temperature superconductivity is not surprising, as 2D-like Cu–O sheets are absent from the structure. Because it is comprised entirely of divalent copper, $La_4Ca_4Cu_8O_{18}$ was found to be insulating. It is likely that the La, Ca contents of both phases can be adjusted over a wide range, with concomitant effects on the hole concentration and electrical properties, but such studies were not carried out.

In order to confirm whether or not the new phases require extreme pressure for synthesis, the preparation of $La_4Ca_4Cu_8O_{20+\delta}$ was attempted at 900°C and pO_2 = 250 bar (in a René steel alloy vessel). The following result was obtained:

$$LaCaCu_2O_{4.5} + 0.25O_2 \rightarrow LaCaCuO_4 + CuO. \quad [2]$$

This was confirmed by directly synthesizing $LaCaCuO_4$ at 900°C and p_{O_2} = 250 bar. X-ray powder diffraction patterns of $LaCaCuO_4$ showed single phase material which could be indexed on the basis of the tetragonal K_2NiF_4 structure with a = 3.7706(6) and c = 13.164(2) Å. The oxygen content of this phase is probably substoichiometric at the pressures used in its preparation. None of the oxygen vessel experiments resulted in the synthesis of $La_4Ca_4Cu_8O_{20+\delta}$.

These results led us to examine an intermediate range of synthesis conditions in the girdle-type apparatus. In experiments at 1025°C and 20–40 kbar pressures, using buffer concentrations equivalent to δ = 0.5–1.0, the following reaction stoichiometry was obtained:

$$1.5\ LaCaCu_2O_5 \rightarrow La_{1.5}Ca_{1.5}Cu_2O_{6+\delta} + CuO. \quad [3]$$

Powder X-ray diffraction pattern of the product could be indexed on the basis of a tetragonal cell with a = 3.8248(6) and c = 19.414(3) Å, corresponding to the known RP phase $La_2CaCu_2O_6$, an intergrowth of perovskite and rock salt layers in a ratio of 2 : 1 (35). This structure consists of double (n = 2) CuO_2 planes separated by a layer of Ca. The $CaCu_2O_4$ units are sandwiched by rock salt layers (La_2O_2). $La_{2-y}Ca_{1+y}Cu_2O_{6+\delta}$ with δ = 0.1–0.3 was also synthesized at 1050°C and 60 kbar by Okai (16), who made it superconducting below 70 K by adjusting the oxygen content with varying amounts of $KClO_3$.

The above results, and related experiments discussed below, suggested the possibility of synthesizing the n = 3 member of the Ruddlesden–Popper series. This compound can be described as an intergrowth of LaO rock salt with three perovskite layers. Accordingly, the compound $La_2Ca_2Cu_3O_{8+\delta}$ was synthesized from the corresponding stoichiometric precursors subjected to high pressure (60 kbar) and a heating sequence consisting of 1–2 hr of reaction at 1025°C followed by annealing at 60 kbar and 750°C for 2–4 hr. The structure of $La_2Ca_2Cu_3O_{8+\delta}$ is shown in Fig. 3. X-ray and electron diffraction show a body-centered tetragonal cell which could be completely indexed in space group $I4/mmm$ with unit cell parameters a = 3.805(1) and c = 27.01(1) Å. The powder X-ray diffraction pattern is given in Table 3.

The preparation of $La_2Ca_2Cu_3O_{8+\delta}$ is very sensitive to experimental conditions. Indeed, the phase was first observed while exploring the possibility of ordering $La_4Ca_4Cu_8O_{20+\delta}$ into the $YBaFeCuO_5$-type structure in 60 kbar annealing experiments at temperatures between 550 and 800°C:

$$2LaCaCu_2O_{5+\delta} \rightarrow La_2Ca_2Cu_3O_{8+\delta} + CuO. \quad [4]$$

Subsequent high pressure work at the nominal stoichiometry $La_2Ca_2Cu_3O_{8+\delta}$, as described above, resulted in its preparation. The annealing conditions following high temperature synthesis was found to be especially crucial. Decomposition products were observed if annealing was

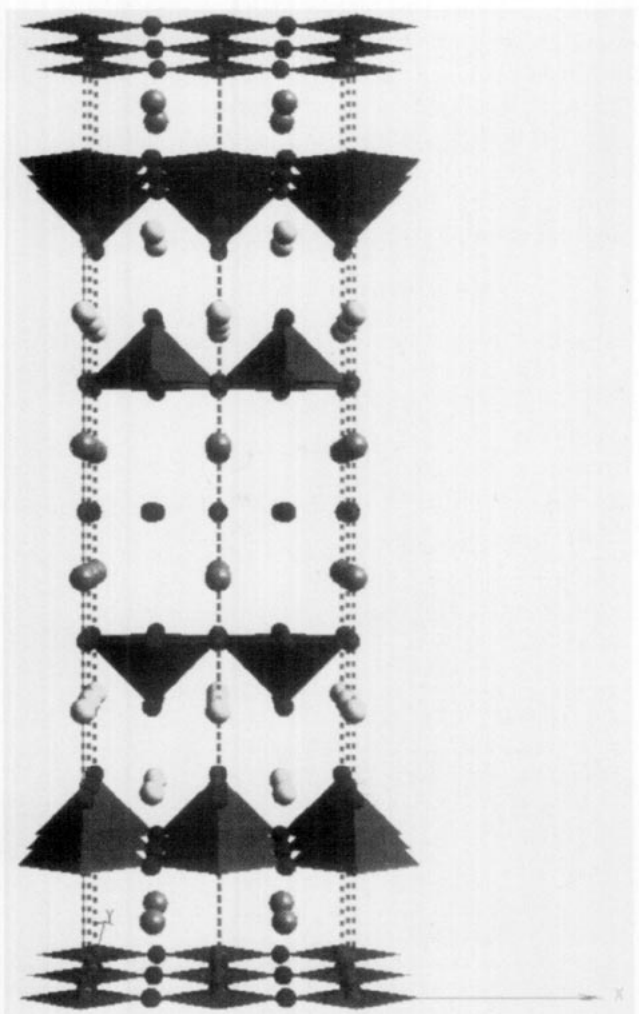

FIG. 3. Three-dimensional representation of the $n = 3$ Ruddlesden–Popper phase $La_2Ca_2Cu_3O_8$. The lightly tinted cations are La, gray cations are calcium, and dark cations are copper and oxygen.

performed at temperatures much above or below 750°C. Moreover, upon quenching from 750°C and 60 kbar, the phase could not be retained for long in the metastable state. Evidence of decomposition into phases amorphous to X-rays was found after as little as 5 days under ambient conditions in a dry box. The tendency toward decomposition at room temperature could be reduced considerably by substituting a fraction of both the La and/or Ca sites with Sr, but the instability of the phase on heating, especially at low pressures, made it very difficult to optimize its hole concentration and oxygen stoichiometry. Therefore, although metallic, $La_2Ca_2Cu_3O_{8+\delta}$ and its Sr-doped analogs have not yet been made superconducting.

The requirement of enhanced pressures for the synthesis of RP polymorphs with higher n was pointed out long ago (36). It is therefore not surprising that the RP $n = 3$ phase has not been prepared in the La–Ca–Cu–O system under ambient conditions. This may be a consequence of the fact that the mismatch between the rock salt and perovskite sheets probably increases with n. Pressure would minimize the mismatch if the inherent stiffness of the perovskite subunit is lower and has a greater pressure dependence than that of the rock-salt layer. Of course, for the same reasons, the $n = 3$ phase would become unstable when quenched to ambient pressure, as observed. Similarly, attempts to synthesize the $n = 4$ phase at pressures up to 60 kbar have also failed. Although it may form at higher pressures, $La_2Ca_3Cu_4O_{10+\delta}$ probably cannot be quenched to ambient pressure. It is interesting to note that RP phases with $n \geq 2$ in the Sr–Cu–O system recently have been quenched from high pressures (37, 38).

There are a number of other interesting aspects to the chemistry of the Ruddlesden–Popper $n = 3$ phase. Most noteworthy is that when the reverse of reaction [4] was run under flowing oxygen (1 atm) up to 650°C in the TGA apparatus (10°C/min), yet another new phase was obtained:

$$1.5La_2Ca_2Cu_3O_{8+y} + 1.5CuO + 0.25O_2 \rightarrow La_3Ca_3Cu_6O_{14+\delta}. \quad [5]$$

The powder X-ray diffraction pattern of the product,

TABLE 3
Powder Diffraction Pattern of $La_2Ca_2Cu_3O_{8+\delta}$
($a = 3.8046(2)$; $c = 26.956(2)$ Å)

d_{obs}	d_{calc}	I_o	I_c	h	k	l
13.50	13.478	10	32	0	0	2
6.710	6.739	5	3	0	0	4
	3.5035	—	9	1	0	3
3.114	3.1085	20	32	1	0	5
2.6985	2.7065	100	100	1	0	7
	2.6956	—	14	0	0	10
2.6901	2.6903	50	53	1	1	0
	2.6382	—	13	1	1	2
	2.4985	—	5	1	1	4
2.2463	2.2463	5	10	0	0	12
	2.1024	—	4	1	1	8
	2.0602	—	4	1	0	11
1.920	1.9254	20	5	0	0	14
	1.9042	7	7	1	1	10
1.900	1.9023	30	35	2	0	0
	1.8836	—	1	2	0	2
1.720	1.7243	15	12	1	1	12
	1.6718	—	2	2	1	3
	1.6226	5	9	2	1	5
1.567	1.5657	10	10	1	1	14
1.555	1.5563	30	32	2	1	7
	1.5542	6	8	2	0	10

TABLE 4
Powder X-Ray Diffraction Pattern of $La_3Ca_3Cu_6O_{14+\delta}$
(a = 5.379(1); c = 11.592(4) Å)

d_{obs}	d_{calc}	I_o	I_c	h	k	l
11.592	11.5922	2	2	0	0	1
3.804	3.8033	5	2	1	1	0
	3.1798	—	2	1	1	2
2.710	2.7106	100	100	1	1	3
2.689	2.6894	50	36	2	0	0
	2.3184	—	2	0	0	5
	2.3051	—	3	1	1	4
2.198	2.2074	—	9	2	0	3
	1.9320	—	11	0	0	6
1.903	1.9017	20	27	2	2	0
1.568	1.5691	15	11	2	0	6
1.555	1.5567	25	30	3	1	3

shown in Table 4, was indexed to a tetragonal cell of the $La_3Ba_3Cu_6O_{14+\delta}$-type, with a = 5.379(1) and c = 11.592(4) Å. This assignment must be considered tentative, however, in view of the fact that several lines of weaker intensity were not observed. If the analogy with $La_3Ba_3Cu_6O_{14+\delta}$ is correct, the structure of $La_3Ca_3Cu_6O_{14+\delta}$ would consist of triple perovskite layers of $ACuO_3$ and an oxygen deficient A-layer (A = La, Ca). The difference between the structure of the n = 3 Ruddlesden–Popper phase and that of the triple perovskite can be visualized by removing the rock-salt slab in the RP phase of the structure of Fig. 3, and ordering the oxygen vacancies accordingly.

SUMMARY AND CONCLUSIONS

The primary focus of this work was to utilize high pressure techniques to synthesize a specific ordered "intergrowth" of perovskite and infinite layer phases, namely, the $YBaFeCuO_5$ structure type. Although the preparation of this phase was not successful, a number of new A-site disordered variants of perovskite were obtained, in addition to a new Ruddlesden–Popper phase with n = 3. These results were realized in a very narrow region of phase space at a cation ratio of 1 : 1 : 2 in the $LaO_{1.5}$–CaO–CuO–O_2 system.

The approach taken, namely, the creation of A-site-disordered perovskites at high pressures, is the first in a series of processing steps required to synthesize the desired ordered phases. High pressures and temperatures provide the driving force required to place A-cations of dissimilar size into similar sites in the same lattice, creating precursor phases which often remain metastable to temperatures in access of 800°C at ambient (and higher) pressures. A wide latitude of annealing conditions can then be explored under controlled P, p_{O_2}, T, to effect conversion of the disordered precursor into new ordered phases. Despite our inability to prepare the desired ordered structures, the richness of the equilibrium and non-equilibrium reaction chemistry observed at the La : Ca : Cu = 1 : 1 : 2 composition is clear evidence of the synthetic potential of this approach. Future work will explore in greater depth the reaction channels taken by these quenched phases at lower temperatures.

ACKNOWLEDGMENT

We thank Dr. David Walker of the Lamont–Doherty Earth Observatory for advice concerning configuring the high pressure sample assembly.

REFERENCES

1. M. Takano, Z. Hiroi, M. Azuma, and Y. Takeda, "Chemistry of High Temperature Superconductors," pp. 243–266. Springer-Verlag, Berlin, 1992.
2. J. B. Goodenough, J. A. Kafalas, and J. M. Longo, *in* "Preparative Methods in Solid State Chemistry" (P. Hagenmuller, Ed.), pp. 1–69. Academic Press, New York, 1972.
3. E. Takayama-Muromachi and A. Navrotsky, *J. Solid State Chem.* **72,** 244 (1988).
4. L.-G. Liu and W. A. Bassett, "Elements, Oxides and Silicates: High Pressure Phases with Implications for the Earth's Interior." Oxford University Press, New York, 1986.
5. M. Takano, Y. Takeda, H. Okada, M. Miyamoto, and T. Kusaka, *Physica C* **159,** 375 (1989).
6. M. Takano, M. Azuma, Z. Hiroi, Y. Bando, and Y. Takeda, *Physica C* **176,** 441 (1991).
7. M. Azuma, Z. Hiroi, M. Takano, Y. Bando, and Y. Takeda, *Nature* **356,** 775 (1992).
8. M. Takano, *in* "Electronic Properties and Mechanisms of High T_c Superconductors" (T. Oguchi, K. Kadowaki, and T. Sasaki, Eds.), pp. 89–94. Elsevier, New York, 1992.
9. A. Ono, *Physica C* **198,** 287 (1992).
10. T. Sakurai, N. Sugii, H. Takizawa, M. Ichikawa, Y. Yaegashi, S. Adachi, M. Shimada, and H. Yamauchi, *Physica C* **193,** 471 (1992).
11. T. Siegrist, S. M. Sahurak, D. W. Murphy, and R. S. Roth, *Nature* **334,** 231 (1988).
12. Z. Hiroi, M. Azuma, M. Takano, and Y. Takeda, *Physica C* **208,** 286 (1993).
13. G. Er, Y. Miyamoto, F. Kanamaru, and S. Kikkawa, *Physica C* **181,** 206 (1991).
14. M. G. Smith, A. Manthiram, J. Zhou, J. B. Goodenough, and J. T. Markert, *Nature* **351,** 549 (1991).
15. W. Korczak, M. Perroux, and P. Strobel, *Physica C* **193,** 303, (1992).
16. B. Okai, *Jpn. J. Appl. Phys.* **30,** L179 (1991).
17. R. J. Cava, B. Batlogg, R. B. van Dover, J. J. Krajewski, J. V. Waszczak, R. M. Fleming, W. F. Peck, L. W. Rupp, P. Marsh, A. C. James, and L. F. Schneemeyer, *Nature* **345,** 602 (1990).
18. Y. Tokura, H. Takagi, and S. Uchida, *Nature* **337,** 335 (1989).
19. J. F. Bringley, S. S. Trail, and B. A. Scott, *J. Solid State Chem.* **86,** 310 (1990).
20. H. Okada, M. Takano, and Y. Takeda, *Physica C* **166,** 111 (1990).
21. P. Bordet, J. J. Capponi, C. Chaillout, D. Chateigner, J. Chenavas, Th. Fournier, J. L. Hodeau, M. Marezio, M. Perroux, G. Thomas, and A. Varela, *Physica C* **193,** 178 (1992).
22. J. F. Bringley, B. A. Scott, S. J. LaPlaca, R. F. Boehme, T. M. Shaw, M. W. McElfresh, S. S. Trail, and D. E. Cox, *Nature* **347,** 263 (1990).

23. J. F. Bringley, B. A. Scott, S. J. LaPlaca, F. Meyran, T. R. McGurie, M. W. McElfresh, and D. E. Cox, *Phys. Rev. B* **47,** 15269 (1993).
24. L. Er-Rakho, C. Michel, Ph. Lacorre, and B. Raveau, *J. Solid State Chem.* **73,** 531 (1988).
25. W. Zhou, P. A. Anderson, C. Lin, and P. P. Edwards, *Physica C* **190,** 59 (1991).
26. L. Barbey, N. Nguyen, V. Caignaert, M. Hervieu, and B. Raveau, *Mater. Res. Bull.* **27,** 295 (1992).
27. P.-E. Werner and H. Treor, "Trial and Error Program for Indexing of Unknown Powder Patterns." Dept. of Structural Chemistry, Arrhenius Laboratory, University of Stockholm, Stockholm, Sweden, 1984.
28. C. M. Clark, D. K. Smith, and G. J. Johnson, "A Fortran IV Program for Calculating X-ray Diffraction Patterns—Version V." Dept. of Geosciences, Penn. State Univ., Univ. Park, PA, 1973.
29. K. Yvon, W. Jeitschko, and E. Parthé, *J. Appl. Crystallogr.* **10,** 73 (1977).
30. Y. U. Kwon and J. D. Corbett, *Chem. Mater.* **2,** 27 (1990).
31. G. Demazeau, C. Parent, M. Pouchard, and P. Hagenmuller, *Mater. Res. Bull.* **I,** 913 (1972).
32. L. Er-Rakho, C. Michel, and B. Raveau, *J. Solid State Chem.* **73,** 514 (1988).
33. C. Michel, L. Er-Rakho, M. Hervieu, and B. Raveau, *J. Solid State Chem.* **68,** 143 (1987).
34. W. T. Fu, Q. Xu, A. A. Verheijen, J. M. van Ruitenbeek, H. W. Zandbergen, and L. J. de Jongh, *Solid State Comm.* **73,** 291 (1990).
35. A. Fuertes, X. Obradors, J. M. Navarro, P. Gomez-Romero, N. Casañ-Pastor, F. Perez, J. Fontcuberta, and C. Miravitlles, *Physica C* **170,** 153 (1990).
36. J. A. Kafalas and J. M. Longo, *J. Solid State Chem.* **4,** 55 (1972).
37. Z. Hiroi, M. Takano, M. Azuma, and Y. Takeda, *Nature* **364,** 315 (1993).
38. S. Adachi, H. Yamauchi, S. Tanaka, and N. Mori, *Physica C* **212,** 164 (1993).